
^{111}In -Labeled Galectin-3–Targeting Peptide as a SPECT Agent for Imaging Breast Tumors

Senthil R. Kumar¹ and Susan L. Deutscher^{1,2}

¹Department of Biochemistry, University of Missouri, Columbia, Missouri; and ²Research Service, Harry S Truman Veterans Memorial Hospital, Columbia, Missouri

Galectin-3 is a member of the galectin family of β -galactoside-binding animal lectins. Galectin-3 is overexpressed in a wide range of neoplasms and is associated with tumor growth and metastases. Given this fact, radiolabeled galectin-3–targeting molecules may be useful for the noninvasive imaging of tumors expressing galectin-3, as well as for targeted radionuclide therapy. In this study, the tumor cell–targeting and SPECT properties of a galectin-3–avid peptide identified from bacteriophage display were evaluated in human breast carcinoma cells and in human breast tumor-bearing mice. **Methods:** The galectin-3–avid peptide G3-C12 (ANTPCGPYTHDCPVKR) was synthesized with a Gly-Ser-Gly (GSG) linker at the amino terminus. After conjugation with 1,4,7,10-tetra-azacyclododecane-*N,N',N''N'''*-tetraacetic acid (DOTA), the peptide was labeled with ^{111}In . The radiochemical purity and stability of the compound was assessed by high-performance liquid chromatography. MDA-MB-435 human breast carcinoma cells expressing galectin-3 were used to characterize the *in vitro* binding properties of the radiolabeled compound. SCID mice bearing MDA-MB-435 xenografts were used as an *in vivo* model for biodistribution and imaging studies with the ^{111}In -labeled peptide. **Results:** ^{111}In -DOTA(GSG)-G3-C12 bound specifically to galectin-3–expressing MDA-MB-435 cells. The radiolabeled peptide was stable in serum and was found intact in excreted urine for at least 1 h. Competitive binding experiments indicated that the radiolabeled peptide exhibited an inhibitory concentration of 50% of 200.00 ± 6.70 nM for cultured breast carcinoma cells. *In vivo* biodistribution studies revealed that tumor uptake was 1.2 ± 0.24 , 0.75 ± 0.05 , and 0.6 ± 0.04 (mean \pm SD) percentage injected dose per gram at 30 min, 1.0 h, and 2.0 h after injection of the radiotracer, respectively. SPECT/CT studies with ^{111}In -DOTA(GSG)-G3-C12 showed excellent tumor uptake and contrast in the tumor-bearing mice. Specificity of peptide binding was demonstrated by successful blocking (52%) of *in vivo* tumor uptake of ^{111}In -DOTA(GSG)-G3-C12 in the presence of its nonradiolabeled counterpart at 2 h after injection. **Conclusion:** This study demonstrated the successful use of a new radiolabeled peptide for the noninvasive imaging of galectin-3–positive breast tumors. This peptide may be a promising candidate for future clinical applications.

Key Words: peptide; phage; galectin-3; imaging; breast cancer

J Nucl Med 2008; 49:796–803

DOI: 10.2967/jnumed.107.048751

Galectin-3 is a member of the galectin family of animal lectins defined by their highly conserved carbohydrate-recognition domain (CRD) and their affinity for β -galactosides (1,2). Galectin-3 is a 30-kDa protein that consists of 3 distinct structural regions: a short 12-amino-acid N terminus leader portion that controls its cellular distribution; a 7- to 10-amino-acid repetitive collagenlike linker; and an approximately 130-amino-acid C terminus domain consisting of the carbohydrate-binding site (1,3,4). Galectin-3 is found not only on the cell surface but also on the cytoplasm and nucleus and can be secreted. The interaction of galectin-3 with various intracellular and extracellular ligands dictates its cellular localization and function (5,6). Importantly, galectin-3 interactions with certain carbohydrates and extracellular matrix proteins facilitate metastasis by promoting tumor cell adhesion and invasion (7), antagonizing tumor cell apoptosis (8,9), and inducing endothelial proliferation and angiogenesis (10). Galectin-3 is expressed in several types of cancer, particularly those of the breast (11,12), and its expression correlates with the transformation and metastasis of many tumor cells *in vivo* (13).

It was previously shown that the cancer-associated Thomsen-Friedenreich antigen (TFA), a Gal β 1–3GalNAc cell surface disaccharide exposed on up to 90% of adenocarcinomas (14), is a major galectin-3 carbohydrate ligand (15). Galectin-3–TFA interaction promotes the redistribution of galectin-3 expressed on endothelial cells to sites of tumor–endothelial cell contact (15), suggesting this lectin–carbohydrate complexation may be a key early step in the formation of intravascular metastases. Thus, studies have focused on the development of inhibitors of galectin-3–TFA interactions for use as antitumor agents. Most such inhibitors have consisted of carbohydrates that bind the CRD of galectin-3 (16). However, these compounds are, in general, not specific for galectin-3 in that they bind other galectin family members via conserved residues in the CRD.

Bacteriophage display was previously used in our laboratory in an effort to obtain peptide-based antagonists of

Received Nov. 1, 2007; revision accepted Jan. 16, 2008.
For correspondence or reprints contact: Susan L. Deutscher, Department of Biochemistry, 117 Schweitzer Hall, 1 Hospital Dr., Columbia, MO 65211.
E-mail: deutschers@missouri.edu
COPYRIGHT © 2008 by the Society of Nuclear Medicine, Inc.

galectin-3 (17). One such peptide, G3-C12 (ANTPCGPYTHDCPVKR), bound with remarkable specificity to galectin-3 but not to other galectin family members or lectins and recognized cell surface galectin-3 expressed on cultured breast carcinoma cells (17). The peptide bound to the C terminus CRD region of galectin-3 and was able to compete for binding to TFA. Furthermore, the galectin-3-targeting peptide inhibited both homotypic adhesion of MDA-MB-435 human breast carcinoma cells and their heterotypic adhesion to endothelial cells. Because of the previously reported accumulation of galectin-3 molecules at the sites of cancer cell interactions (15), we hypothesized that the galectin-3-targeting peptide may form the basis for an imaging agent to monitor tumor growth and metastasis in vivo. In the present study, we examined whether a radiolabeled version of the G3-C12 peptide could be used as a SPECT/CT agent for galectin-3-expressing human breast tumors heterotransplanted into mice. To this end, G3-C12 peptide was conjugated, via a Gly-Ser-Gly (GSG)-linker sequence, to the radiometal chelator 1,4,7,10-tetra-azacyclododecane-*N,N',N''N'''*-tetraacetic acid (DOTA). The peptide conjugate was radiolabeled with ^{111}In and analyzed for binding to cultured MDA-MB-435 human breast carcinoma cells. The biodistribution properties of the ^{111}In -DOTA(GSG)-ANTPCGPYTHDCPVKR peptide and its ability to perform as a SPECT agent were explored in vivo in mice bearing human MDA-MB-435 breast tumors.

MATERIALS AND METHODS

Chemicals and Reagents

Amino acids and resin were purchased from Advanced Chem-Tech. DOTA-tri-*t*-butyl ester was purchased from Macrocylic, Inc. $^{111}\text{InCl}_3$ was purchased from Mallinckrodt Chemicals. All other reagents in this study were obtained from Fisher Scientific Co. unless otherwise specified.

Cell Lines and Cell Culture

Human breast carcinoma cell line MDA-MB-435 was obtained from American Type Tissue Culture. BT549 human breast carcinoma cell line was provided by Dr. Avraham Raz (Karmanos Cancer Institute). The cells were maintained as monolayer cultures in RPMI-1640 medium supplemented with 10% fetal bovine serum, sodium pyruvate, nonessential amino acids, and L-glutamine. Cultures were maintained at 37°C in a 5% CO_2 humidified incubator. Subculturing was performed using standard procedures.

Peptide Synthesis

Peptides were synthesized in a model 396 multiple peptide synthesizer (Advanced Chem Tech) using solid-phase Fmoc chemistry. For radiolabeling, the chelator DOTA was coupled to the NH_2 terminus of linear G3-C12 (ANTPCGPYTHDCPVKR) or a scrambled peptide version (PPPKGDVHTNRTYACC) with a GSG amino acid spacer between DOTA and the NH_2 terminus alanine or proline of the peptide. Peptides were purified using reverse-phase high-pressure liquid chromatography (RP-HPLC) on a C18 column (218TP54; Vydac), lyophilized, and stored at -20°C before use. Identities of the peptides were confirmed by electrospray ionization mass spectrometry (Mass Consortium Corp.).

Peptide Radiolabeling

The ^{111}In -labeling of DOTA(GSG)-ANTPCGPYTHDCPVKR (G3-C12) or DOTA(GSG)-PPPKGDVHTNRTYACC (scrambled version of G3-C12) was performed essentially as previously described (18). Briefly, the peptides were radiolabeled with ^{111}In by incubating 25 μg of peptide in 5 μL of $^{111}\text{InCl}_3$ (185 MBq/500 μL) (Mallinckrodt) and 80 μL of ammonium acetate, pH 5.5, at 85°C for 60 min, after which 10 μL of 2 mM ethylenediamine tetraacetic acid were added to complex unreacted ^{111}In . The radiolabeled peptide conjugate was purified by RP-HPLC (10%–95% acetonitrile/0.1% trifluoroacetic acid) for 30 min. Purified preparations were flushed with nitrogen gas to remove acetonitrile, and the pH was adjusted to neutral by adding 0.2 M sodium phosphate and 0.15 M NaCl, pH 8.0.

Peptide Stability

The stability of the radiolabeled peptide conjugate was analyzed in 0.01 M phosphate-buffered saline (PBS) containing 0.1% bovine serum albumin, pH 7.4, at 37°C for various times (1, 2, 4, 6, and 12 h) and monitored for degradation by HPLC. Stability was also tested in mouse serum by incubating 11.1 MBq of ^{111}In -DOTA(GSG)-G3-C12 in 500 μL of serum at 37°C for 30 min, 1 h, and 2 h, respectively. Afterward, the samples were centrifuged at 12,500 rpm, and 20- μL aliquots of the supernatant were analyzed by RP-HPLC.

Urinary Metabolites of ^{111}In -DOTA(GSG)-G3-C12

One hundred fifty microliters of HPLC-purified ^{111}In -DOTA(GSG)-G3-C12 (3.70–5.55 MBq) were injected into MDA-MB-435 human breast cancer cell-bearing SCID mice through the tail vein, and urine was collected at 30, 60, and 120 min later. The radioactive metabolites in the urine were analyzed by RP-HPLC using a 20-min gradient of 25%–90% acetonitrile/0.1% TFA.

In Vitro Cell Binding of ^{111}In -DOTA(GSG)-G3-C12

Experiments to test the ability of the radiolabeled peptide to bind breast carcinoma cells known either to express galectin-3 (MDA-MB-435) or not to express galectin-3 (BT549) were performed. Cells grown in culture flasks were trypsinized, released, and washed once in cell-binding medium (RPMI 1640 with 25 mM *N*-2-hydroxyethylpiperazine-*N*-2-ethanesulfonic acid, pH 7.4, 0.2% bovine serum albumin, and 3 mM 1,10-phenanthroline). Cells (1×10^6 cells per tube) were transferred to small microcentrifuge tubes containing 0.3 mL of cell-binding medium and were incubated at 37°C for different times (15 min and 0.5, 0.75, 1.0, 1.5, and 2 h) with 2×10^4 cpm of radiolabeled peptide. After incubation, the medium was removed and the cells were rinsed with ice-cold 0.01 M PBS, pH 7.4, and 0.2% bovine serum albumin and were centrifuged. This process was repeated 2 more times. Radioactivity bound to the cells was quantitated in a Wallac γ -counter (PerkinElmer Life and Analytic Sciences Inc.). Cell-binding ability was reported as total radioactivity (cpm) that was bound to the cells. As a negative control, cell-binding experiments were also performed with a radiolabeled scrambled G3-C12 peptide, DOTA-(GSG)-PPPKGDVHTNRTYACC.

Competition experiments were performed with radiolabeled DOTA-(GSG)-G3-C12 peptide along with its nonradiolabeled counterpart to determine the ligand concentrations that inhibited 50% of the maximum specific binding (IC_{50}) to the cancer cells. MDA-MB-435 human breast carcinoma cells (1×10^6 cells per tube) were incubated with 2×10^4 cpm of ^{111}In -DOTA(GSG)-G3-C12 peptide and different concentrations (10^{-4} – 10^{-13} M) of the non-radioactive indium-DOTA(GSG)-G3-C12 peptide in 0.3 mL of

cell-binding medium at 37°C. Cells were then pelleted by centrifugation and the supernatant removed. The cell pellet was washed twice with 0.5 mL of ice-cold binding buffer, and the radioactivity in the pellet was measured in a γ -counter. IC₅₀ values for the peptide were calculated using Graft software (Erithacus Software Limited).

Internalization Experiments

Internalization of the radiolabeled peptide into MDA-MB-435 human breast carcinoma cells was analyzed at 37°C. Cells (1×10^6 /tube) were incubated with ¹¹¹In-DOTA(GSG)-G3-C12 (2.5×10^4 cpm) and were pelleted after 15 min, 30 min, 1 h, 1.5 h, and 2 h. Cell pellets were washed twice with ice-cold cell-binding medium to remove any unbound activity and further rinsed in 1.2% cold acetic acid, pH 2.5, containing saline, stirred in a vortex mixer, and incubated for 5 min on ice. Cells were pelleted by centrifugation. The supernatant, which contained the surface-bound peptide, was collected. Radioactivity in both the supernatant and the cell pellet (internalized radioactive peptide) was measured in a γ -counter.

Biodistribution Studies

All animal studies were conducted in accordance with the Guide for the Care and Use of Laboratory Animals (19) and the policy and procedures for animal research at the Harry S Truman Veterans Memorial Hospital. Female 4- to 6-wk-old SCID (ICR SCID) mice were obtained from Taconic. The mice received a subcutaneous implant of 1×10^7 MDA-MB-435 human breast carcinoma cells in the shoulder. Mice (3 per time point) were injected with approximately 0.11 MBq (2.71×10^{-15} M peptide) of the ¹¹¹In-DOTA(GSG)-G3-C12 peptide through the tail vein and were housed separately after administration of radioactivity. The mice were sacrificed by cervical dislocation at 15 min and 1, 2, 4, and 24 h after injection, after which tissues and organs of interest were collected. Gastrointestinal tract contents were not removed. The animal, tissue, and organ samples were weighed, and counts were determined with an automated γ -counter. The total blood volume was calculated as 6.5% of the whole-body weight. Uptake of radioactivity in the tumor and normal tissues and organs was expressed as a percentage of the injected radioactive dose (%ID) per gram or as %ID of tissue.

For blocking experiments, the tumor mice were preinjected with 100 μ g of DOTA(GSG)-G3-C12 peptide labeled with 1×10^{-4} M nonradioactive indium. After 15 min postinjection of the nonradiolabeled peptide, 0.11 MBq of radiolabeled counterpart was injected, and the blocking efficiency was evaluated after 2 h. Statistical comparisons between groups were performed by the unpaired Student *t* test. A *P* value of 0.05 or less was considered statistically significant.

Small-Animal SPECT/CT Studies

Breast tumor (MDA-MB-435) xenografts were established by injecting 1×10^7 cells in the shoulder region of SCID mice. Radiolabeled peptide scintigraphy was performed by injecting 11.1 MBq (2.71×10^{-13} M peptide/100 μ L) of ¹¹¹In-DOTA(GSG)-G3-C12 peptide into the tail vein of the mice. After 2 h after injection, the mice were euthanized with carbon dioxide and imaged at the Biomolecular Imaging Center at the Harry S Truman Veterans Memorial Hospital using a MicroCAT II (Siemens Medical Solutions) dedicated small-animal SPECT/CT scanner equipped with a high-resolution 2-mm pinhole collimator. The volumetric voxel image matrix data were reconstructed using a 3-dimensional ordered-subset expectation maximization algorithm. Planar whole-

body imaging was performed, and the images were reconstructed using a fanbeam (Feldkamp) filtered-backprojection algorithm. Radiolabeled peptide SPECT images were fused with CT images to validate regions of increased radiolabeled ligand uptake. Coregistered SPECT and CT data were visualized using Amira 3.1 software (TGS). A similar imaging study was performed with radiolabeled scrambled G3-C12 peptide ¹¹¹In-DOTA(GSG)-PPKGDVHTNRTYACC.

Statistical Analysis

The data were expressed as mean \pm SD. Mean values were compared using the Student *t* test.

RESULTS

Radiolabeling

DOTA(GSG)-ANTPCGPYTHDCPVKR G3-C12 peptide and DOTA(GSG)-PPKGDVHTNRTYACC G3-C12 scrambled peptide were synthesized and purified by RP-HPLC. A GSG spacer was introduced between the DOTA and the NH₂ terminus of the peptides to avoid potential steric hindrance. The peptides were successfully labeled with ¹¹¹InCl₃ in ammonium acetate buffer (pH 5.5) at 85°C for 1 h. The radiolabeled peptides were purified to homogeneity by C18 RP-HPLC. The radiolabeled peptide eluted at 13.5 min, and the nonradiolabeled counterpart eluted at 12.3 min. Radiolabeling efficiency was 50%–60%. The radiochemical purity of the peptide was more than 98% when rechecked by HPLC. The radiolabeling yield after purification was 30%, with a high specific activity (68.45 GBq/ μ mol). Similarly, radiolabeled ¹¹¹In-DOTA(GSG)-PPKGDVHTNRTYACC scrambled peptide was separated by RP-HPLC from its nonradiolabeled counterpart.

Peptide Stability

The stability of the ¹¹¹In-DOTA(GSG)-G3-C12 radiolabeled peptide in 0.01 M PBS, pH 7.4, was examined. The radiolabeled peptide was radiochemically stable for 12 h in PBS, as determined by RP-HPLC analysis. RP-HPLC was also used to analyze the metabolic stability of the radiolabeled peptide incubated in mouse serum for different intervals (Fig. 1). The peptide conjugate was stable in both serum (85% \pm 8.0%) and urine (80% \pm 6.0%) at 30 min after injection; however, some degradation was found at later times.

In Vitro Cell Binding

It was important to ascertain whether the radiolabeled DOTA-peptide conjugates retained binding affinity for galectin-3. In vitro cell-binding experiments were thus performed with ¹¹¹In-DOTA(GSG)-G3-C12 and MDA-MB-435 human breast carcinoma cells known to express high levels (~ 10 ng/mg protein) of galectin-3 (7,17,20). These cells are also tumorigenic in animals and serve as a good model of human breast tumors for imaging studies (21). The galectin-3-binding ability of the radiolabeled peptides to MDA-MB-435 human breast carcinoma cells was analyzed in vitro by incubating radiolabeled peptide conjugate (2×10^4 cpm) with MDA-MB-435 carcinoma cells (1×10^6 cells per well) for various times at 37°C. Binding of the

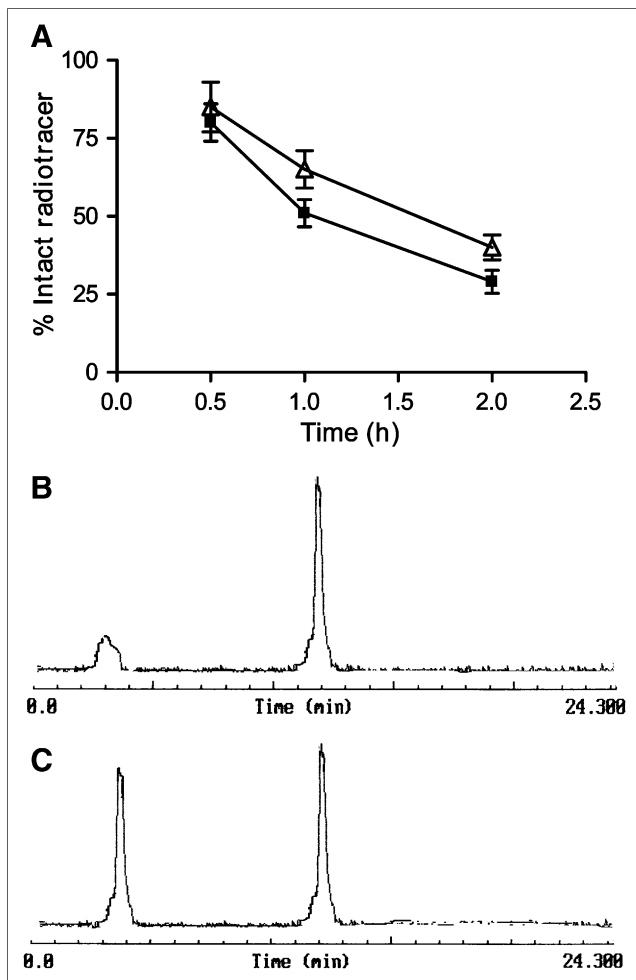


FIGURE 1. Stability of ^{111}In -DOTA(GSG)-ANTPCG-PYTHDCPVKR in biologic fluids. (A) Time course of intact tracer in serum (Δ) and urine (\blacksquare). (B and C) Representative HPLC elution profiles of radiotracer in urine (B) and serum (C) collected after 1 h of incubation at 37°C after *in vitro* or *in vivo* tracer injection, respectively. In both cases, most of the radiotracer was intact at end of 1 h.

^{111}In -DOTA(GSG)-G3-C12 peptide to the cells increased gradually, leveling off by 2 h. No significant increase in binding was observed after that time, indicating saturable binding of the peptide to the cells. A cell-binding capacity of about 5% was obtained for the G3-C12 peptide with respect to the initial total radioactivity added to the MDA-MB-435 carcinoma cells (Fig. 2). Similar studies with BT549 human breast carcinoma cells that are galectin-3-negative (22) did not show appreciable binding of ^{111}In -DOTA(GSG)-G3-C12, indicating that the radiolabeled peptide was specific for galectin-3-expressing human breast cancer cells. The radiolabeled G3-C12 scrambled peptide ^{111}In -DOTA(GSG)-PPPKGDVHTNRTYACC did not bind either cell line.

The specificity of binding of the ^{111}In -DOTA(GSG)-G3-C12 galectin-3-avid peptide to MDA-MB-435 breast carcinoma cells was determined by competition experiments in the presence of various concentrations of nonradioactive indium-

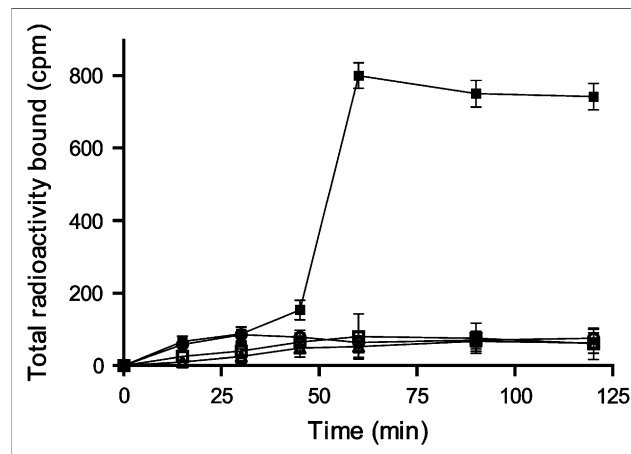


FIGURE 2. Galectin-3-binding properties of ^{111}In -DOTA(GSG)-ANTPCG-PYTHDCPVKR. Approximately 1.0×10^6 cells per well were incubated at 37°C for different intervals with 2×10^4 cpm of ^{111}In -DOTA(GSG)-ANTPCG-PYTHDCPVKR. Although significant radioligand binding to human MDA-MB-435 breast carcinoma cells was observed (\blacksquare), minimal binding was observed with galectin-3-negative BT-549 breast cancer cells (\circ). Little binding of radiolabeled G3-C12 scrambled peptide [^{111}In -DOTA(GSG)-PPPKGDVHTNRTYACC] was observed with MDA-MB-435 (\square) or BT-549 (Δ) cell lines.

DOTA(GSG)-G3-C12 peptide. Binding of the peptide to the breast carcinoma cells decreased in a concentration-dependent manner in the presence of the nonradiolabeled counterpart, as indicated by a decrease in bound radioactivity (Fig. 3). Analysis of the binding data indicated that the radiolabeled ^{111}In -DOTA(GSG)-G3-C12 exhibited an IC_{50} value for

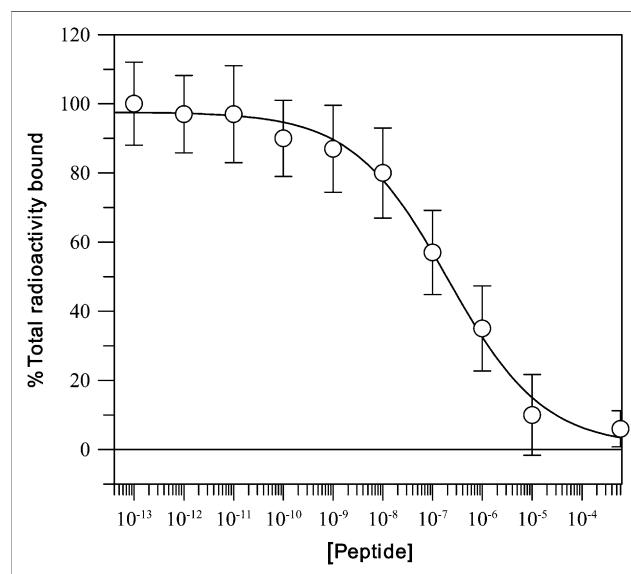


FIGURE 3. Displacement of ^{111}In -DOTA(GSG)-ANTPCG-PYTHDCPVKR peptide by its nonradiolabeled counterpart. MDA-MB-435 cells (1×10^6) were incubated with 2×10^4 cpm of radioligand and increasing concentrations of nonradioactive peptide (10^{-13} – 10^{-4} M). IC_{50} was 200.00 ± 6.70 nM. Each data point represents mean \pm SD of 3 replicates.

MDA-MBA-435 breast carcinoma cells of 200.00 ± 6.70 nM. Cell internalization studies indicated no radioactivity inside the cells.

In Vivo Biodistribution Studies

The biodistribution of the ^{111}In -DOTA(GSG)-G3-C12 peptide was examined in female SCID mice bearing MDA-MB-435 human breast tumors. The tumor and organ distribution of the radiolabeled peptide at 30 min and 1, 2, 4, and 24 h after injection is shown in Table 1. Tumor uptake of the radiolabeled peptide was 1.20 ± 0.75 %ID/g, 0.75 ± 0.05 %ID/g, and 0.60 ± 0.04 %ID/g at 30 min, 1 h, and 2 h, respectively, indicating tumor retention of the radiolabeled ligand. Radioactive levels in the blood were 1.69 ± 0.45 %ID/g 30 min after injection, followed by a rapid clearance by the end of 2 h (0.07 ± 0.01 %ID/g). Rapid tumor uptake and blood clearance kinetics resulted in a tumor-to-blood ratio of 8.6 at the end of 2 h, a value 12 times higher than the ratio (0.70) obtained after 30 min after injection. Whole-body disappearance of radioactivity was equally rapid, with 65.6 %ID in the urine 30 min after injection and 88.6 %ID after 1 h. High tumor-to-blood and tumor-to-muscle uptake ratios were demonstrated as early as 1 h after injection (Table 1). Normal-organ uptake of radioactivity was highest in the kidneys, as they were the primary route of excretion. Radioactivity in the kidneys declined from a peak of 30.6 ± 4.48 %ID/g 30 min after injection to 25.9 ± 1.56 %ID/g at 1 h and 22.3 ± 4.32 %ID/g at the end of 4 h. Excluding the kidneys, only the lungs exhibited any appreciable retention of radio-

activity. Lung radioactivity was 1.50 ± 0.26 %ID/g 30 min after injection, decreasing to 0.23 ± 0.02 %ID/g at 2 h, which was below the 2-h tumor value (0.60 ± 0.04 %ID/g). Little radioactivity was retained in the remaining vital organs, muscle, or bone.

The specificity of tumor uptake of the radiolabeled ^{111}In -DOTA(GSG)-G3-C12 peptide in vivo was further evaluated by performing competition experiments with its unlabeled counterpart (Table 1). MDA-MB-435 tumor mice ($n = 3$) were injected via the tail vein with nonradioactive indium-DOTA(GSG)-G3-C12 peptide followed 15 min later by injection of its radioactive ^{111}In -peptide counterpart. As a positive control, another set of mice ($n = 3$) was simultaneously injected with only the radiolabeled peptide. The results, shown in Figure 4, indicate that the tumor uptake of radiolabeled peptide was blocked by about 52% in mice injected with the nonradioactive peptide ($P = 0.01$). The presence of excess nonradioactive peptide did not affect the percentage of radioactivity uptake per gram of tissue in the normal organs, including the lungs and kidneys.

SPECT/CT Tumor Imaging

The tumor imaging efficacy of ^{111}In -DOTA(GSG)-ANTPCGPYTHDCPVKR G3-C12 was evaluated in SCID mice bearing galectin-3-expressing MDA-MB-435 human breast tumors. A whole-body SPECT/CT scan was performed at 2 h after injection. A representative image is shown in Figure 5A. The breast tumor was clearly visualized, with high tumor-to-background contrast for the tracer. The

TABLE 1
Pharmacokinetics of ^{111}In -DOTA(GSG)-ANTPCGPYTHDCPVKR

Tissues	30 min	1 h	2 h	2-h block	4 h	24 h
%ID/g						
Tumor	1.20 ± 0.75	0.75 ± 0.05	0.60 ± 0.04	0.31 ± 0.07	0.16 ± 0.04	0.07 ± 0.01
Brain	0.05 ± 0.02	0.01 ± 0.00	0.01 ± 0.00	0.01 ± 0.00	0.00 ± 0.00	0.00 ± 0.00
Blood	1.69 ± 0.45	0.31 ± 0.05	0.07 ± 0.01	0.07 ± 0.02	0.04 ± 0.00	0.01 ± 0.01
Heart	0.62 ± 0.19	0.13 ± 0.02	0.04 ± 0.01	0.04 ± 0.00	0.03 ± 0.00	0.03 ± 0.00
Lung	1.50 ± 0.26	0.49 ± 0.03	0.23 ± 0.02	0.21 ± 0.03	0.13 ± 0.01	0.06 ± 0.01
Liver	0.61 ± 0.14	0.25 ± 0.02	0.20 ± 0.03	0.22 ± 0.05	0.17 ± 0.01	0.16 ± 0.03
Spleen	0.49 ± 0.09	0.16 ± 0.01	0.08 ± 0.01	0.12 ± 0.03	0.07 ± 0.00	0.10 ± 0.00
Kidneys	30.60 ± 4.48	25.90 ± 1.56	22.30 ± 5.06	21.80 ± 2.80	22.30 ± 4.32	12.30 ± 2.43
Muscle	0.31 ± 0.11	0.06 ± 0.01	0.02 ± 0.00	0.02 ± 0.01	0.01 ± 0.00	0.02 ± 0.01
Pancreas	0.61 ± 0.20	0.13 ± 0.04	0.03 ± 0.00	0.02 ± 0.00	0.02 ± 0.01	0.02 ± 0.01
Bone	0.24 ± 0.06	0.07 ± 0.01	0.02 ± 0.08	0.03 ± 0.01	0.02 ± 0.00	0.05 ± 0.02
%ID						
Stomach	0.20 ± 0.52	0.06 ± 0.02	0.05 ± 0.04	ND	0.01 ± 0.00	0.00 ± 0.00
Intestines	1.08 ± 0.29	0.52 ± 0.18	0.51 ± 0.03	ND	0.48 ± 0.06	0.25 ± 0.02
Urine	65.60 ± 12.40	88.60 ± 0.60	91.90 ± 1.02	ND	92.90 ± 1.50	95.90 ± 0.60
Uptake ratio						
Tumor to blood	0.70	2.40	8.60	ND	4.00	7.00
Tumor to muscle	3.80	12.50	30.00	ND	16.00	3.50

ND = not determined.

Data are presented as %ID/g or %ID (mean \pm SD), or as uptake ratio of tumor to normal tissue, for female SCID mice ($n = 3$) bearing MDA-MB-435 breast xenografts sacrificed at different time points after tail vein administration of ^{111}In -DOTA(GSG)-ANTPCGPYTHDCPVKR.

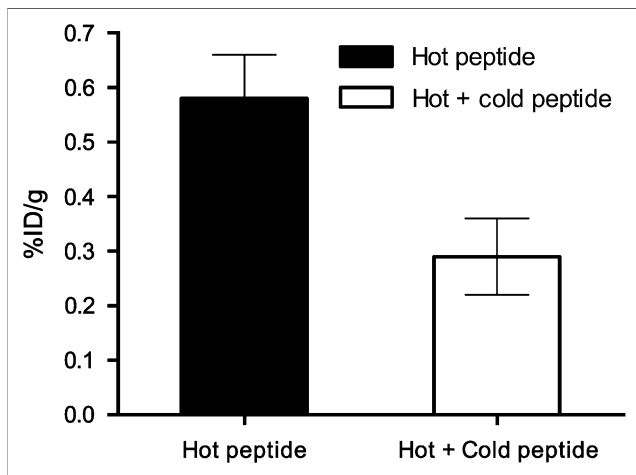


FIGURE 4. In vivo blocking studies with In-DOTA(GSG)-ANTPCGPYTHDCPVKR in MDA-MB-435 breast tumor-xenografted SCID mice. After 15 min after injection of nonradiolabeled In-DOTA(GSG)-ANTPCGPYTHDCPVKR peptide, 0.11 MBq of radiolabeled counterpart was injected, and blocking efficiency was evaluated after 2 h. A 52% block of radiolabeled peptide binding to tumor tissue was observed. Data represent mean \pm SD of 3 animals for each experiment ($P < 0.001$).

high radioactive uptake in the kidneys was coincident with the pharmacokinetics of the radiolabeled peptide (Table 1). Similar studies with the scrambled peptide ^{111}In -DOTA(GSG)-PPPKGDVHTNRTYACC showed no uptake in the tumor (Fig. 5).

Radiotracer accumulation was not significant in the remaining organs, indicative of rapid whole-body clearance of the administered radioactive peptide. These results suggest that tumor uptake was specific for the galectin-3-targeting G3-C12 (ANTPCGPYTHDCPVKR) peptide, and the radioactivity in the kidneys was nonpeptide-specific.

DISCUSSION

Elevated galectin-3 expression significantly enhances tumor cell adhesion to extracellular matrix proteins (11), increases the incidence of lung metastases (23), and protects cancer cells from apoptosis (9,24). These observations suggest that galectin-3 expression and its interactions with its cognate carbohydrate ligands are important in tumor metastasis. Galectin-3 is highly expressed on endothelial cells and on carcinoma cells such as those of the breast (12). Galectin-3 expressed on endothelial cells interacts with the carbohydrate ligand TFA on carcinoma cells to mediate tumor cell adhesion and metastasis (15,25). On stimulation with TFA-containing glycoproteins, endothelial galectin-3 rapidly redistributes to the sites of tumor cell-endothelial cell contacts (15,25), suggesting that galectin-3/TFA interactions are important early steps in the formation of intravascular metastatic deposits. Inhibiting these steps could potentially modify metastasis-associated tumor cell adhesion and help control metastatic cancer spread. Numerous carbohydrate-based antagonists that bind the CRD of galectin-3 have been

developed and have shown promise in inhibiting galectin-3/carbohydrate-mediated cancer cell adhesion in vitro and in animal models of cancer (16,23,25,26). We previously identified peptides from bacteriophage display selections that block galectin-3-mediated adhesion and TFA interaction (17). These peptides bind to a unique region of galectin-3 and may thus offer greater specificity than the carbohydrate-based inhibitors. Although galectin-3 is expressed in many cell types and in many cell locations, its increased expression and redistribution to sites of cancer cell contacts would indicate that a galectin-3-targeting peptide, once radiolabeled, may serve as a valuable cancer imaging agent in vivo. Hence, the goal of this study was to determine whether the bacteriophage display-selected peptide G3-C12 (ANTPCGPYTHDCPVKR), once radiolabeled with γ -emitting ^{111}In , could act as a galectin-3-mediated SPECT agent in a mouse model of human breast cancer.

The DOTA(GSG)-G3-C12 peptide was synthesized and efficiently radiolabeled with ^{111}In . ^{111}In -DOTA(GSG)-ANTPCGPYTHDCPVKR bound well to galectin-3-positive MDA-MB-435 breast carcinoma cells, whereas binding to nogalectin-3-expressing breast carcinoma cells (BT549) was negligible. Binding was sequence-specific in that a radiolabeled scrambled peptide variant of G3-C12 (^{111}In -DOTA(GSG)-PPPKGDVHTNRTYACC) did not bind the

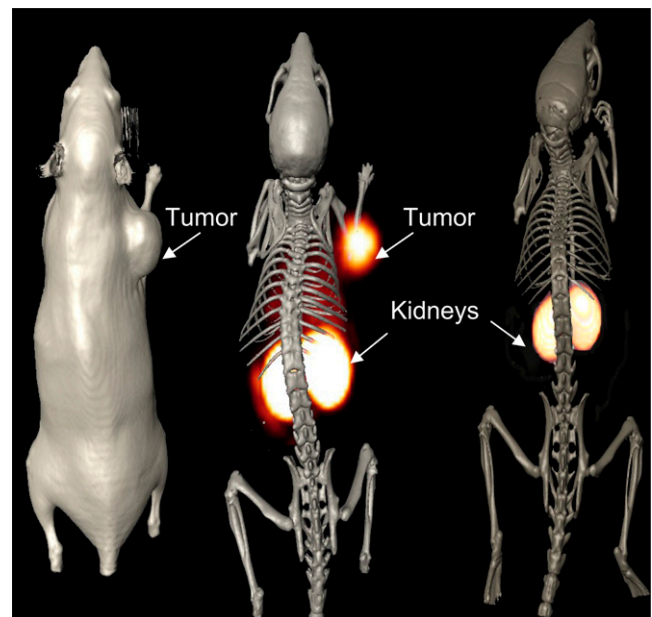


FIGURE 5. Tumor imaging with ^{111}In -DOTA(GSG)-ANTPCGPYTHDCPVKR peptide. MDA-MB-435 breast tumor-xenografted SCID mice were injected in tail vein with 11.1 MBq of ^{111}In -DOTA(GSG)-ANTPCGPYTHDCPVKR peptide and imaged in MicroCAT II (Siemens Medical Solutions) dedicated small-animal SPECT/CT scanner equipped with high-resolution 2-mm pinhole collimator. SPECT images were fused with conventional CT images to validate regions of increased radiolabeled ligand uptake. At left is volume-rendered CT image; at center, coregistered SPECT/CT radioligand uptake image of galectin-3-avid peptide; and at right, SPECT/CT image of scrambled peptide. Imaging was performed 2 h after injection.

carcinoma cells. Competition studies with unlabeled peptide demonstrated specificity of the radiolabeled peptide for the breast carcinoma cells. Radiolabeled peptide binding occurred on the cell surface, and no internalization of the peptide was observed. This result is consistent with the finding that galectin-3 translocates to the cell surface in well-differentiated microvessels of metastasis-prone tissues in response to activation by TFA (23). ^{111}In -DOTA(GSG)-G3-C12 peptide exhibited an IC_{50} of 200.00 ± 6.70 nM for MBA-MB-435 cultured breast carcinoma cells in competitive binding experiments. This binding affinity is comparable to the previously reported affinity of G3-C12 of 88.0 ± 23.0 nM for recombinant galectin-3, as determined by fluorescence quenching titration (17).

The inherent stability of the ^{111}In -DOTA(GSG)-G3-C12 peptide was tested in vitro in PBS and serum and in vivo in urine. The radioconjugate was found to be stable in buffer, serum, and urine for at least 1 h. Degradation of the radiolabeled peptide after 1 h in serum could be attributed to the presence of plasma peptidases. Because the chemically synthesized peptide contained only natural amino acids, some degree of proteolysis might be expected. However, the original peptide sequence was selected on filamentous bacteriophage as a fusion to a stable coat protein and therefore was likely protected against proteolysis (17,27).

In vivo evaluation of ^{111}In -DOTA(GSG)-G3-C12 indicated rapid and specific targeting of galectin-3-expressing human breast tumor xenografts. The clearance of free radioactivity was quick and occurred exclusively via the urinary tract, with most of the retained radioactivity being in the kidneys. Nonspecific accumulation of radioactivity in the kidneys is often associated with the in vivo application of radiolabeled peptides (28). The molecular mechanism of renal uptake of radiolabeled peptides is not completely understood. High levels of accumulation of radiolabeled polypeptides in the kidneys may be due to the long residence time of radiometabolites produced by lysosomal degradation within renal cells (29–31). Increased renal uptake could also be attributed to the presence of lysine (32,33), free sulfhydryls, or disulfide bonds in the polypeptide (34). Strategies to decrease renal uptake, including infusion of basic amino acids or diuretics, may help to reduce renal uptake of the ^{111}In -DOTA(GSG)-G3-C12 peptide in the future (35,36). However, previous studies reported that radiolabeled peptide uptake in the kidneys can be reduced by amino acid infusions before injection of the peptide, and such procedures reduced the radiolabeled peptide accumulation by only 40% (36,37). Nevertheless, nonspecific retention of radioactivity in other organs, including the hepatobiliary system, was low.

Because of the rapid blood clearance of the galectin-3-avid peptide, tumor-to-blood ratios increased steadily over time and reached high values ($>8.6:1$) by 2 h. In vivo scintigraphic imaging studies with ^{111}In -DOTA(GSG)-G3-C12 revealed a high tumor uptake in mice with MDA-MB-435 human breast carcinoma xenografts. Radiotracer accumulation was predominantly in the tumor and kidneys.

Insignificant whole-body, hepatobiliary, or minimal radioactivity in the lungs was observed, indicating the potential of this novel radiotracer for in vivo tumor imaging.

The development of bacteriophage display-selected peptide-based imaging agents has centered primarily on the vascular endothelial component, $\alpha_v\beta_3$ -integrin, targeting RGD peptide or its derivatives (38–40). Few other bacteriophage-selected peptides that bind tumor-associated antigens have been reported to function as efficacious tumor imaging agents in vivo. Recently, we successfully used an ErbB-2 receptor-targeting peptide (KCCYSL), derived from a bacteriophage display library, for SPECT/CT of human xenografted breast tumors in mice (18). Here, we demonstrated that ^{111}In -DOTA(GSG)-G3-C12 can be used to image galectin-3-expressing MDA-MB-435 human breast cancer xenografts in SCID mice. Our studies imply that cancer cell-associated imaging agents, in addition to vasculature-targeting imaging agents, can be developed from bacteriophage display-selected peptides. These tumor-associated peptide-based imaging vehicles may be useful in advancing an individualized approach to cancer detection and treatment.

CONCLUSION

The stability, biodistribution, and imaging properties of the galectin-3-targeting ^{111}In -DOTA (GSG)-ANTPCG-PYTHDCPVKR G3-C12 peptide were evaluated. High tumor uptake and retention, coupled with whole-body clearance in MDA-MB-435 human breast tumor-bearing SCID mice, suggest that this peptide has potential as a radiopharmaceutical for imaging of galectin-3-expressing tumors, including those of the breast.

ACKNOWLEDGMENTS

We acknowledge the contributions of Lisa Watkinson, Terry Carmack, Marie T. Dickerson, Said Daibes Figueroa, and Thomas P. Quinn. This work was supported in part by a Merit Review Award from the Veterans Administration and by NIH P50 CA103130-01.

REFERENCES

1. Barondes SH, Cooper DN, Gitt MA, Leffler H. Galectins: structure and function of a large family of animal lectins. *J Biol Chem.* 1994;269:20807–20810.
2. Raz A, Lotan R. Endogenous galactoside-binding lectins: a new class of functional tumor cell surface molecules related to metastasis. *Cancer Metastasis Rev.* 1987;6:433–452.
3. Seetharaman J, Kanigsberg A, Slaaby R, Leffler H, Barondes SH, Rini JM. X-ray crystal structure of the human galectin-3 carbohydrate recognition domain at 2.1-Å resolution. *J Biol Chem.* 1998;273:13047–13052.
4. Morris S, Ahmad N, Andre S, et al. Quaternary solution structures of galectins-1, -3, and -7. *Glycobiology.* 2004;14:293–300.
5. Gong HC, Honjo Y, Nangia-Makker P, et al. The NH2 terminus of galectin-3 governs cellular compartmentalization and functions in cancer cells. *Cancer Res.* 1999;59:6239–6245.
6. Nakahara S, Oka N, Wang Y, Hogan V, Inohara H, Raz A. Characterization of the nuclear import pathways of galectin-3. *Cancer Res.* 2006;66:9995–10006.
7. Inohara H, Raz A. Functional evidence that cell surface galectin-3 mediates homotypic cell adhesion. *Cancer Res.* 1995;55:3267–3271.

8. Matarrese P, Fusco O, Tinari N, et al. Galectin-3 overexpression protects from apoptosis by improving cell adhesion properties. *Int J Cancer*. 2000;85:545–554.
9. Fukumori T, Oka N, Takenaka Y, et al. Galectin-3 regulates mitochondrial stability and antiapoptotic function in response to anticancer drug in prostate cancer. *Cancer Res*. 2006;66:3114–3119.
10. Nangia-Makker P, Honjo Y, Sarvis R, et al. Galectin-3 induces endothelial cell morphogenesis and angiogenesis. *Am J Pathol*. 2000;156:899–909.
11. Ochieng J, Warfield P, Green-Jarvis B, Fentie I. Galectin-3 regulates the adhesive interaction between breast carcinoma cells and elastin. *J Cell Biochem*. 1999;75:505–514.
12. Idikio H. Galectin-3 expression in human breast carcinoma: correlation with cancer histologic grade. *Int J Oncol*. 1998;12:1287–1290.
13. Takenaka Y, Fukumori T, Raz A. Galectin-3 and metastasis. *Glycoconj J*. 2004;19:543–549.
14. Springer GF. T and Tn, general carcinoma autoantigens. *Science*. 1984;224:1198–1206.
15. Glinsky VV, Glinsky GV, Rittenhouse-Olson K, et al. The role of Thomsen-Friedenreich antigen in adhesion of human breast and prostate cancer cells to the endothelium. *Cancer Res*. 2001;61:4851–4857.
16. Nangia-Makker P, Hogan V, Honjo Y, et al. Inhibition of human cancer cell growth and metastasis in nude mice by oral intake of modified citrus pectin. *J Natl Cancer Inst*. 2002;94:1854–1862.
17. Zou J, Glinsky VV, Landon L, Matthews L, Deutscher SL. Peptides specific to the galectin-3 carbohydrate recognition domain inhibit metastasis-associated cancer cell adhesion. *Carcinogenesis*. 2005;26:309–318.
18. Kumar SR, Quinn TP, Deutscher SL. Evaluation of an ¹¹¹In-radiolabeled peptide as a targeting and imaging agent for ErbB-2 receptor expressing breast carcinomas. *Clin Cancer Res*. 2007;13:6070–6079.
19. *Guide for the Care and Use of Laboratory Animals*. Washington, DC: National Academy Press; 1996.
20. Khaldoyanidi SK, Glinsky VV, Sikora L, et al. MDA-MB-435 human breast carcinoma cell homo- and heterotypic adhesion under flow conditions is mediated in part by Thomsen-Friedenreich antigen-galectin-3 interactions. *J Biol Chem*. 2003;278:4127–4134.
21. Price JE, Polyzos A, Zhang RD, Daniels LM. Tumorigenicity and metastasis of human breast carcinoma cell lines in nude mice. *Cancer Res*. 1990;50:717–721.
22. Kim HR, Lin HM, Biliran H, Raz A. Cell cycle and inhibition of anoikis by galectin-3 in human breast epithelial cells. *Cancer Res*. 1999;59:4148–4154.
23. Pienta KJ, Naik H, Akhtar A, et al. Inhibition of spontaneous metastasis in a rat prostate cancer model by oral administration of modified citrus pectin. *J Natl Cancer Inst*. 1995;87:348–353.
24. Akahani S, Nangia-Makker P, Inohara H, Kim H-RC, Raz A. Galectin-3: a novel antiapoptotic molecule with a functional BH1 (NWGR) domain of Bcl-2 family. *Cancer Res*. 1997;57:5272–5276.
25. Glinskii OV, Turk JR, Pienta KJ, Huxley VH, Glinsky VV. Evidence of porcine and human endothelium activation by cancer-associated carbohydrates expressed on glycoproteins and tumor cells. *J Physiol*. 2004;554:89–99.
26. Johnson KD, Glinskii OV, Mossine VV, et al. Galectin-3 as a potential therapeutic target in tumors arising from malignant endothelia. *Neoplasia*. 2007;9:662–670.
27. Askoxylakis V, Zitzmann S, Mier W, et al. Preclinical evaluation of the breast cancer cell-binding peptide p160. *Clin Cancer Res*. 2005;11:6705–6712.
28. Lang L, Jagoda E, Wu C, et al. Factors influencing the in vivo pharmacokinetics of peptides and antibody fragments: the pharmacokinetics of two PET-labeled low molecular weight proteins. *Q J Nucl Med*. 1997;41:53–61.
29. Tsai SW, Li L, Williams LE, Anderson A-L, Raubitschek AA, Shively JE. Metabolism and renal clearance of ¹¹¹In-labeled DOTA-conjugated antibody fragments. *Bioconjug Chem*. 2001;12:264–270.
30. Franano FN, Edwards WB, Welch MJ, Duncan JR. Metabolism of receptor targeted ¹¹¹In-DTPA-glycoproteins: identification of ¹¹¹In-DTPA-ε-lysine as the primary metabolic and excretory product. *Nucl Med Biol*. 1994;21:1023–1024.
31. Rogers BE, Franano FN, Duncan JR, et al. Identification of metabolites of ¹¹¹In-diethylenetriaminepentaacetic acid-monoconal antibodies and antibody fragment in vivo. *Cancer Res*. 1995;55(suppl):5714s–5720s.
32. Morgenson CE, Sølling K. Studies on renal tubular protein reabsorption: partial and near complete inhibition by certain amino acids. *Scand J Clin Lab Invest*. 1977;37:477–486.
33. Silbernagl S. The renal handling of amino acids and oligopeptides. *Physiol Rev*. 1988;68:911–1007.
34. Chen J, Cheng Z, Owen NK, et al. Evaluation of an ¹¹¹In-DOTA-rhenium cyclized α-MSH analog: a novel cyclic-peptide analog with improved tumor-targeting properties. *J Nucl Med*. 2001;42:1847–1855.
35. Behr TM, Sharkey RM, Juweid ME, et al. Reduction of the renal uptake of radiolabeled monoclonal antibody fragments by cationic amino acids and their derivatives. *Cancer Res*. 1995;55:3825–3834.
36. Valkema R, de Jong M, Kooij PPM, Kwekkeboom D, Krenning EP. Effective and safe inhibition of renal uptake of radiolabeled peptides by combined lysine and arginine infusion [abstract]. *J Nucl Med*. 2001;42(suppl):37P.
37. Rolleman EJ, Valkema R, de Jong M, Kooij PP, Krenning EP. Safe and effective inhibition of renal uptake of radiolabelled octreotide by a combination of lysine and arginine. *Eur J Nucl Med Mol Imaging*. 2003;30:9–15.
38. Arap W, Pasqualini R, Ruoslahti E. Cancer treatment by targeted drug delivery to tumor vasculature in a mouse model. *Science*. 1998;279:377–380.
39. Arap W, Kolonin MG, Trepel M, et al. Steps toward mapping the human vasculature by phage display. *Nat Med*. 2002;8:121–127.
40. Haubner R, Wester HJ. Radiolabeled tracers for imaging of tumor angiogenesis and evaluation of anti-angiogenic therapies. *Curr Pharm Des*. 2004;10:1439–1455.